Assessment of a Vehicle's Electromagnetic Emissions Under Dynamic Drive Conditions

Konstantinos Pliakostathis, Marco Zanni, Germana Trentadue, and Harald Scholz

***Abstract*—This article presents measured results carried out inside an automotive EMC semianechoic chamber of test methodologies that assess the radiated emissions of a plug-in hybrid vehicle (PHEV) under dynamic drive conditions including acceleration, deceleration and different constant speeds. On the contrary, existing automotive EMC test methods applied as per UNECE Regulation 10 and CISPR 12, concerning the radiated emissions of vehicles, consider fixed laboratory setups and vehicle drive conditions. Test parameters, such as 360° azimuth scan around the vehicle, antenna height scan and broadband versus fixed-frequency measurement techniques based on a single vehicle demonstrate that actual radiated emissions can be higher than those in fixed laboratory configurations prescribed on existing standards. Next to this, measurements that associate the time-dependence of the electromagnetic emissions with vehicle's parameters such as velocity and power from the (electric) traction battery are analyzed and discussed. Furthermore, results of radiated emissions below 30 MHz and above 1 GHz, which are not obligatory during vehicle EMC testing, are outlined. The EMC test methodologies discussed in this work can assist the EMC troubleshooting of vehicles and help to quickly identify the critical area(s) around the vehicle that contribute to the generated electromagnetic interference.**

***Index Terms*—Automotive EMC standards, electromagnetic interference (EMI), plug-in hybrid vehicle (PHEV), vehicle radiated emissions.**

I. Introduction

THIS article discusses the results of an extensive number of EMC laboratory tests of a plug-in hybrid vehicle (PHEV) under dynamic and realistic driving conditions and multiple EM-reception configurations in order to understand the level of the radiated emissions such a vehicle can generate. The measured data was produced at the Vehicle Emissions Laboratory (V*e*LA) 9 automotive EMC semianechoic chamber (SAC) of the European Interoperability Centre for Electric Vehicles and Smart Grids at the Joint Research Centre of the European Commission. We demonstrate that the radiated emissions, based on current automotive EMC vehicle type approval methods [1], [2] can turn out different and particularly higher under more complex—but day to day relevant—driving conditions.

A typical vehicle nowadays employs a large number of switching-mode circuits, wires, and sensors to control and coordinate numerous functions, which can introduce unwanted parasitic capacitances and inductances within the vehicle's subsystems [3]. Excessive EM emissions from vehicles expose systems to quality, availability, reliability [4], and functional safety [5] issues and as well raise concerns related to the exposure of humans to EM radiation, e.g., [6]. We believe that the findings presented in this work can as well contribute to the EMC troubleshooting and debugging process of a vehicle, which is particularly critical in today's automotive tests.

Currently, very limited number of papers in the literature have attempted to present systematic automotive EMC measurement procedures, but none reflects modern vehicles. Based on actual laboratory data, we indicate that current EMC automotive test methods can underestimate or miss the worst-case EM emissions when dynamic driving and steady mode conditions under different setups are considered. The results presented here are only exemplary and aim to show the radiated emissions from a typical PHEV vehicle of today's globalized market and add to the basis for further discussion into the formulation and development of EMC automotive test methods and approaches that give a higher degree of certainty in the level of EM emissions and EMC vehicle troubleshooting.

In the European Union currently UNECE Regulation No. 10 (Nov. 20, 2019) [1] governs the EMC procedures for the type approval of road vehicles, which replaced the Automotive EMC Directive [7]. Within this regulation, the measurement methods for the radiated emissions of the whole vehicle are conducted according to CISPR 12:2001+AMD1:2005 [8] both, for the broadband and narrowband emissions. At the time of writing, the latest version of CISPR 12 was CISPR 12:2007 complemented with the minor amendment included on AMD1:2009 CSV [2], which discarded the broadband/narrowband distinction, but is leaving the test method intact. Therefore, it is almost a decade ago since a base-giving standard for the EM emissions approval of vehicles was updated. We are concerned whether this leaves a gap, which has the potential to miss issues that most recent vehicle technology can pose with regard to the electromagnetic interference (EMI). In addition to this, some simplifying aspects of the test methods considered within the current automotive standards may indeed not reflect the reality well. Such considerations have been reported, e.g., in [9]–[12].

Manuscript received July 16, 2019; revised October 14, 2019 and December 18, 2019; accepted December 30, 2019. Date of publication March 23, 2020; date of current version December 14, 2020. *(Corresponding author: Konstantinos Pliakostathis.)*

The authors are with the Joint Research Centre of the European Commission, Directorate C, Energy, Transport and Climate, Sustainable Transport, 1755 ZG, Petten, The Netherlands (e-mail: konstantinos.pliakostathis@ec.europa.eu; marco.zanni@ec.europa.eu; germana.trentadue@ec.europa.eu; harald.scholz@ec.europa.eu).

Color versions of one or more of the figures in this article are available online at http://ieeexplore.ieee.org.

Digital Object Identifier 10.1109/TEMC.2020.2968140

A. Issues With the Current CISPR 12 Test Methods

The current version of CISPR 12 considers two modes of the vehicle during the test; they are: 1) Key-ON, Engine OFF and 2) Engine running.

On "Key-ON, Engine OFF" the ignition is switched ON, in case of fuel combustion engine. It is not clear however how this is precisely linked to battery-based, fully electric or PHEVs, where there is no "ignition," but rather an active closed-circuit formed involving already the vehicle's propulsion battery system. On the other hand, the "engine running condition" requires the test then to be carried out only at a constant speed of 40 km/h, and when inside a SAC, with a dynamometer without a load [12].

As well known, CISPR 12 tests for EM emissions regarding vehicle compliance are prescribed in the frequency range between 30 and 1000 MHz. Yet, radiated emissions can extend over this frequency range [13], [14] due to the onboard electronic circuitry of modern vehicles. For example, the powertrain and high-power modules employed for the management of the electrical engines on EVs and PHEVs utilize high-speed pulsewidth-modulation signals which can produce strong EMI beyond 30–1000 MHz [15]–[17]. Furthermore, vehicle connectivity with other portable devices can rely on 2.4 GHz band or 5G technology (e.g., 3.5, 5.9 GHz). Hence, there is a concern that electromagnetic emissions from a vehicle could easily spread outside the original CISPR 12 frequency range with the potential to cause unwanted interference to a plethora of other wireless services [27].

Current test approval procedures prescribe that the setup of the receive antenna with respect to the vehicle should be fixed. In particular:

1) A fixed antenna height is required (3 or 1.8 m for 10 and 3 m distance, respectively, from the vehicle)
2) The EM emissions are measured in fixed positions on the left and right side of the vehicle.

The aforementioned methods, related to the radiated emissions, are well established for many years and have been applied by the automotive industry. They have gained a high degree of maturity across the EMC test laboratories globally and are simple to apply. However, the fact that these have never been changed for more than a decade raises questions regarding their effective coverage of today's technological developments and thus, effects.

Section II presents our alternative test methods going beyond CISPR 12 on pre-normative purpose, and give a description and reasoning of the factors upon which these were chosen. After this, the laboratory results, Section III, as generated inside our automotive electromagnetic SAC of V*e*LA 9, are presented and analyzed next to a brief discussion on the measurement challenges. Section IV provides conclusions around our work and suggestions for future initiatives proposed.

II. Test Setup and Measurement Procedures for Vehicle Radiated Emissions

In principle, there are numerous test setups and drive conditions that can be applied in a laboratory. As very often in the industry, also in our case the test vehicle was only for a limited amount of days at disposition for EMC testing. For this reason, it was crucial to define an optimized test methodology in order to reduce test times and maximize the radiated emissions under more realistic drive scenarios. This allowed to provide a qualitative and quantitative understanding of the emissions that the proposed test methods could reveal and compare them with those foreseen by the current EMC regulation.

A. Measurement Detector Selection

CISPR 12 allows to carry out initial frequency scans with the EMI receiver instrument set to peak detector, while the quasi-peak is also allowed as an alternative option e.g., in "Engine-Running" mode. Among the two types of detectors, the peak has the fastest response time as it reacts almost instantly to the peak level of the measured signal, while the quasi-peak detector has a slower charge and discharge time during signal acquisition [4], [20]. Additionally, the use of the quasi-peak detector requires a measurement (or dwell) time of 1 s, while the peak detector 5 ms so it covers a full frequency sweep 200 times faster. For this reason, next to the objective to carry out direct pre-normative EMC assessment of the vehicle, the peak detector with maximum-hold was employed for the measurements in order to reduce test times and reach the first-order conclusion of the frequencies that are challenging the emissions limit.

B. Test Parameters for the Examination of Radiated Emissions Under Dynamic Drive Conditions

It is arguable that especially in urban and congested areas like city centers, motorists very rarely drive at constant speed for a prolonged period. Apparently, constant velocity can only cover a small part of the whole trip in urban areas as in most cases the vehicle continuously has to accelerate and decelerate to adapt, e.g., to the traffic, road signs and traffic lights. Except for cruise-controlled driving on flat and straight highways, even on higher speed roads, it is rare to retain a constant speed for several seconds. Microadjustments on the pedal are always required to keep the speed, not to consider the presence of turns and slopes affecting the speed. So, driving only at one constant speed during the assessment of EMC vehicle emissions departures considerably from the reality. Therefore in this work not only different drive speed levels but also accelerations and decelerations were investigated in terms of their EM emissions.

Furthermore, the gearbox of the vehicles is increasingly managed by more advanced electric circuitry, replacing gradually the conventional mechanical functionalities. This raises the concern as to whether EM disturbances can be generated during its operation. Such a factor was considered in our test methods as well.

CISPR 12 considers fixed antenna height and vehicle configurations (i.e., left and right side) during testing. In reality, radio frequency disturbances can take place all around the vehicle, as with any electronic device [11]; so a full 360° scan around the vehicle should be necessary. In addition, antenna height scanning could also be a crucial parameter for the maximization of the captured EM exposure caused the vehicle. This is an approach, which is widely known on other instances of the

TABLE I
TEST PARAMETERS CONSIDERED FOR REAL DRIVE CONDITIONS

Test Variable	Value
Vehicle velocity	40, 60, 80, 100, 120 km/h
Drive mode	Stationary and ON Acceleration phase Constant speed Deceleration phase (breaking or freewheeling)
Frequency range	150 kHz - 30 MHz (RBW = 9 kHz) 30 - 1000 MHz (RBW = 120 kHz) 1 - 6 GHz (RBW = 1 MHz)
EMI receiver mode	Frequency Domain (with FFT) and/or Fixed Frequency (single frequency)
Antenna height	From 1.5m to 3.0m in steps of 0.5m
Vehicle azimuth rotation angle	0 to 360 degrees under vehicle speed

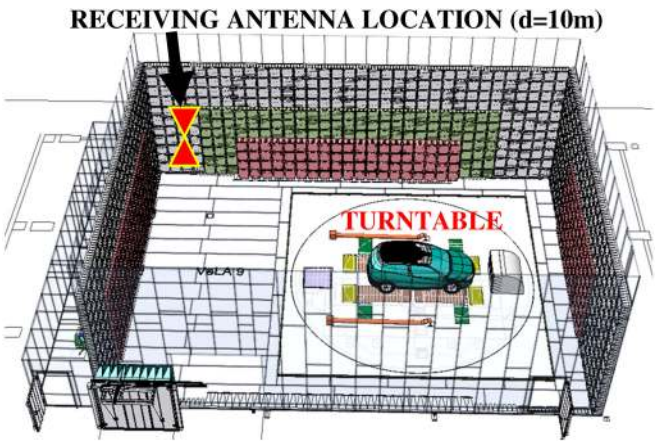

Fig. 1. Computer visualization of the EMC SAC (ceiling removed to expose the interior).

EMC certification of a product, e.g., CISPR 32 [18], which has replaced CISPR 22 [19].

Table I, lists the main test variables which were taken into account in the measurement methods presented in this work, with the aim to get nearer to realistic driving and environment conditions as much as possible inside an EMC chamber.

C. Vehicle, Automotive EMC Semianechoic Chamber, and Antenna Setup

The PHEV in consideration was tested only in pure electric drive mode during speed, while the display in front of the driver's seat was providing instantaneous information about the state of operation and vehicle parameters, such as battery state of charge, level of regeneration or battery consumption, speed, etc., Table VI (Appendix), outlines the vehicle's technical specifications.

Fig. 1 illustrates the layout of the test facility while Table VII (Appendix) describes the EMC equipment used for the tests. The use of a SAC, instead of an open test area ensured that external interferences were absent during the measurements. The dimensions of the SAC, used for this pre-normative study, were 21 × 15.6 × 8.0 m (length × width × height) and hence allowed the placing of the antenna at 10 m from the vehicle to minimize field variations due to antenna radiation pattern. The same SAC incorporated a 11 m in diameter turntable, where the vehicle was fixed using nonconductive straps specially tailored for EMC tests and undergone a full 360° rotation with vehicle tyres touching the metallic rollers. The SAC's turntable had four independently controlled roller chassis dynamometer cylinder motors that allowed to drive the vehicle up to 210 km/h weighting 4 ton maximum, with the option to accelerate and decelerate within values of up to 10 m/s^2. In front of the vehicle, there was a ventilation system tailored to emulate the air flow during driving. The SAC has been validated in accordance with CISPR 16-1-4 [21] for Reference Site Method and site VSWR (10 m and up to 18 GHz) not exceeding ±3 and 6 dB, respectively.

The receiving antennas were placed 10 m away from the vehicle, at a height of 3 m (nonconductive antenna mast) for the broadband antenna and at 1.2 m (nonconductive tripod) for the active monopole antenna above the metallic surface of the SAC.

For the purpose of matching real road conditions, physical parameters were incorporated on the chassis dynamometer system to simulate the inertia of the vehicle, actual road load resistance and effect of air-drag on the chassis of the vehicle. Table VIII (Appendix) outlines these parameters, obtained by means of a coast down procedure based on New European Driving Cycle (NEDC) road load [22].

D. Analysis of Radiated Emissions Measurement Protocols

Given the limited time of availability of the vehicle to be tested inside our EMC chamber, representative drive test protocols were defined in order to optimize the number of tests and the procedure required to carry out each test. The purpose of these test protocols was to acquire results that compare the radiated emissions as defined on the standards, with the results produced under more real drive conditions. The tests were broken down into the following segments:

1) Full 360° azimuth scans of the vehicle at various constant speeds during broadband frequency sweep. This allowed to identify the most critical frequency across a frequency band and relate to the level of EM emissions with respect to vehicle speed.
2) Full 360° azimuth scan of the vehicle at various constant speeds at a fixed frequency to identify the critical angle in terms of the emissions from the vehicle.
3) Constant speed, vehicle acceleration and deceleration instances at a fixed observation angle, captured with the scan receiver set either: 1) in frequency domain (FD) (with FFT) or 2) at fixed frequency to observe the field variations in time.
4) Execution of a complete drive cycle in order to reproduce inside the laboratory a typical real drive situation, which includes: switch-ON, gear set (P-R-N-D), acceleration, constant speed, deceleration, gear set, switch-OFF in the FD and/or at fixed frequency.

After the initial pre-scan, the critical frequencies identified were measured over a narrower frequency span that matched the receiver's maximum fast-Fourier transform (FFT) band [23], [24] as this ensured that emissions could be maximized. The FFT

TABLE II
APPLIED TEST METHODS TO IDENTIFY THE ACTUAL RADIATED EMISSIONS DURING REAL DRIVE CONDITIONS

Outline of Test Methods	Vehicle Status	Scope
1. 360 rotation in frequency domain (FD)	Constant speed (40, 60, 80, 100, 120 km/h)	Identify critical frequency
2. 360 rotation at fixed frequency	Constant speed (40, 60, 80, 100, 120 km/h)	Identify critical angle
3. Emissions in FD during full drive cycle (multiple constant speeds)	Various (stepped) constant speeds between 40 and 120 km/h, including the accelerations	Identify the impact of different constant speeds and the effect of the intermediate accelerations and final deceleration
4. Emissions in FD during full drive cycle (one constant speed)	Constant speed	Identify impact of relatively aggressive accelerations and decelerations
5. Full drive cycle at fixed frequency	Real drive conditions (switch-ON, set gears, acceleration, constant speed, deceleration, set gears, switch-OFF)	Associate electric field emissions with vehicle operations in time
6. Reverse driving in the frequency domain	Constant speed	Identify impact of reverse driving

process in the FD provides a parallel and simultaneous capturing of multiple frequency bins on a given band, thus providing significant time reductions, avoiding the requirement to scan progressively from one frequency to the next, as it happens on traditional sweep mode spectrum analyzers [25]. The use of time domain receivers (i.e., FFT-based) is foreseen to be incorporated on the next edition of CISPR 12 (edition 7) [26].

Based on the discussion above, Table II, provides an outline of the test methods presented in this work as conducted in our laboratory. The proposed test methodologies aimed to provide a practical guidance on the identification of the worst case emissions of a vehicle either in steady (constant speed or idle mode) or dynamic conditions (acceleration, deceleration, and gear-box operation). A detailed analysis for each of the test methods described on Table II follows next.

Test method 1, in Table II, captured the highest level of the radiated emissions in the FD around the vehicle at constant speed and fixed antenna height, during a complete 360° rotation. Identification of the critical frequency (or frequencies) was noted down at the completion of this test method.

On test method 2, the measurement receiver was set to acquire the emissions in time while the frequency was fixed at the critical frequency of the test method 1. During the measurement, the vehicle was driven at a constant speed on the chassis dynamometer, while the turntable executed one full rotation of 360° at constant angular speed. After the end of the measurement, a data mapping, between: 1) angle of the turntable and 2) capture time, allowed to visualize the radiation pattern of the electric field (E-field)emitted around the vehicle for a fixed antenna height. This provided immediate identification of the most critical viewing angle (or angles) around the vehicle. With the information of the critical frequency and critical angle, it was then possible to gain an understanding of the worst-case emission level under constant vehicle speed.

TABLE III
INTERMEDIATE INSTANCES DURING A DRIVE CYCLE AT STEPPED SPEEDS UP TO 120 KM/H ("NORMAL ACCELERATION": ACCELERATOR WAS KEPT PRESSED 50% OF ITS MAXIMUM REACH, WHILE BRAKE WAS PRESS UP TO 50% OF ITS MAXIMUM REACH)

Stepped Speed Drive Cycle (test method 3)
1. Switch-ON and gear-D
2. Accelerate to 40 km/h
3. Retain 40 km/h
4. Accelerate from 40 to 60 km/h
5. Retain 60 km/h
6. Accelerate from 60 to 80 km/h
7. Retain 80 km/h
8. Accelerate from 80 to 100 km/h
9. Retain 100 km/h
10. Accelerate from 100 to 120 km/h
11. Retain 120 km/h
12. Decelerate from 120 to 0 km/h
13. Gear-out and switch-OFF

TABLE IV
INTERMEDIATE STEPS FROM 0 TO 80 KM/H ACCELERATION CYCLE ("ACCELERATION": ACCELERATOR WAS FULLY PRESSED UP TO ITS MAXIMUM REACH, WHILE BRAKE WAS FULLY PRESSED UP TO 100% OF ITS MAXIMUM REACH)

Stepped Speed Drive Cycle (test method 4)
1. Switch-ON and gear-D
2. Accelerate from 0 km/h to 80 km/h
3. Retain 80 km/h
4. Decelerate from 80 km/h to 0 km/h
5. Gear-out and switch-OFF

Test method 3 considered several intermediate drive scenarios to explore actual conditions more closely. In this method, the vehicle remained on a fixed angle with respect to the antenna, which was also fixed in height, while it was driven in a stepped manner, from idle into higher speeds ranging between 40 and 120 km/h. The purpose of this test block was to evaluate the vehicle's broadband radiated emissions at different speeds during a full drive cycle and to examine the potential impact of minor speed increments, i.e., accelerations, between these different speeds. Hence, it consisted of several intermediate sections in order for us to evaluate in greater detail the level of the radiated emissions under more complex and dynamic drive scenarios.

More specifically, a complete drive cycle of method 3 required to capture and save 13 different instances using the EMI receiver instrument in the FD for a given laboratory setup. Table III gives a detailed description of the test blocks during the test method 3. During each intermediate constant speed, the radiated emissions were measured with the EMI receiver executing multiple sweeps across the band for at least 60 s in order to maximize the capture of the emissions.

Test method 4, aimed to identify the effect that more aggressive speed changes, i.e., accelerations and decelerations, could have on the radiated emissions. The intermediate steps of this test method are presented on Table IV.

Test method 5, was carried out with the test receiver locked at a fixed frequency within a fixed resolution bandwidth (RBW), i.e., 120 kHz, while the level of the radiated emissions was examined as a function of time. During this test the vehicle was driven on a complete drive-cycle, to include all events under

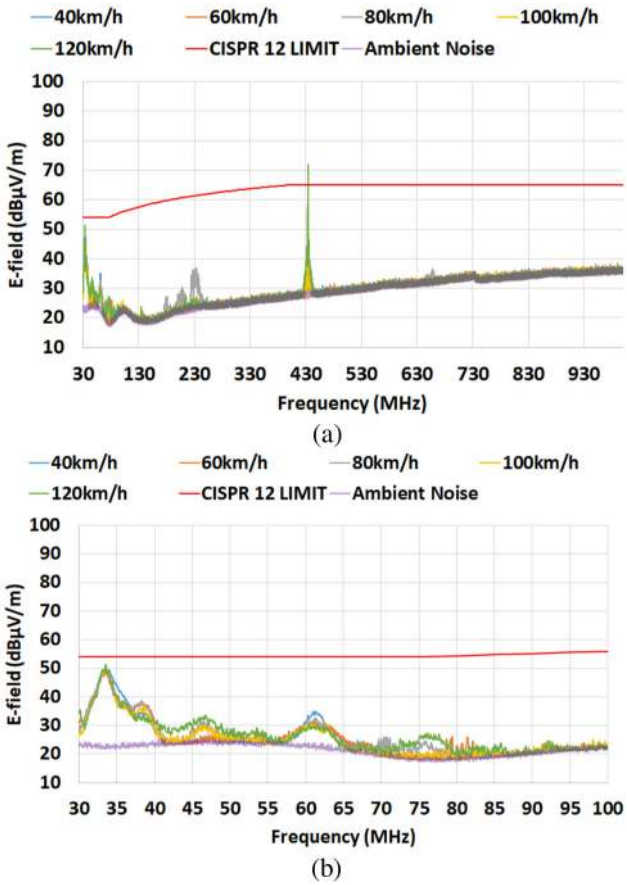

Fig. 2. Worst-case E-field emissions around the vehicle at different constant speeds (vertical polarization) for frequency span. (a) 30–1000 MHz. (b) 30–100 MHz.

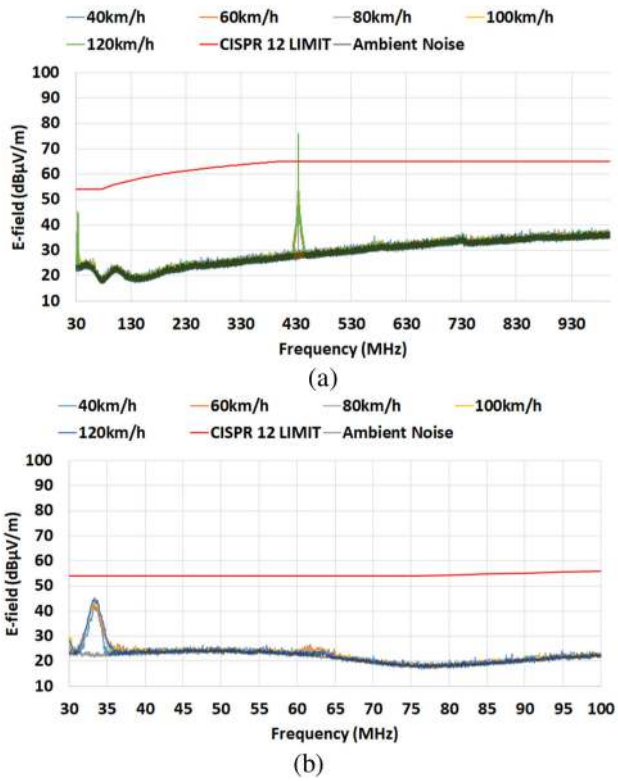

Fig. 3. Worst-case E-field emissions around the vehicle at different constant speeds (horizontal polarization) for frequency span. (a) 30–1000 MHz. (b) 30–100 MHz.

typical real-life conditions: switching-ON, setting of the gears, acceleration, driving at a constant speed, deceleration, re-set the gears, and switch-OFF of the engine. Together with this time analysis, the power consumed (or produced by regeneration) from the (electric) traction battery and the velocity of the vehicle, were recorded in parallel in order to examine their association with the level of the radiated emissions.

Finally, test method 6, considered the investigation of the EM emissions during reverse driving.

III. Laboratory Results and Analysis

A. Impact of Different Constant Speeds

In this test block, we examined the dependence of the highest E-field emitted during a full 360° azimuth scan around the vehicle when the vehicle was driven at different constant speeds of 40, 60, 80, 100, and 120 km/h. The results with the receive antenna at fixed 3 m distance from the ground in vertical polarization are shown in Fig. 2.

From Fig. 2(a), the major EM disturbances during different constant speeds appeared at around 33.48 and 433.9 MHz. However, only the former frequency at 33.48 MHz was attributed to the emissions due to the powertrain of the vehicle during driving. The narrowband frequency at 433.9 MHz was an emission generated by an onboard electronic module of the vehicle, as described in the manufacturers operating manual, which was active during motion. Hence, for the purpose of our investigation, only the 33.48 MHz was relevant, although the 433.9 MHz introduced a consideration from the EMC point of view as it had exceeded the allowed radiated limit defined by the relevant automotive EMC standard. The level of emissions for the horizontal polarization are shown in Fig. 3(a) and the worst E-field close to 33 MHz was generally lower by about 5 dB compared to the vertical polarization.

From Fig. 2(b) it is seen that different constant speeds resulted in minor deviations on the radiated emissions, which were peaking close to 51 dB at 120 km/h in the worst-case emissions situation for the vertical polarization. However, observation of the 30–100 MHz band in the horizontal polarization, Fig. 3(b), revealed that the level of EM emissions was a stronger function of the vehicle's velocity with the E-field deviating progressively as much as 5 dB from 40 to 120 km/h.

The results observed from 30 to 1000 MHz in Figs. 2 and 3 identified that the major EMI was mainly concentrated around 33.48 MHz during speed. For the sake of the discussions in this article we will call this the "critical" frequency. This frequency will be used as the basis for further analysis of the radiated emissions in the following sections.

B. Radiation Pattern Under Constant Vehicle Velocity

Based on the extraction of the critical frequency identified on the previous section, we carried out a full 360° rotation around

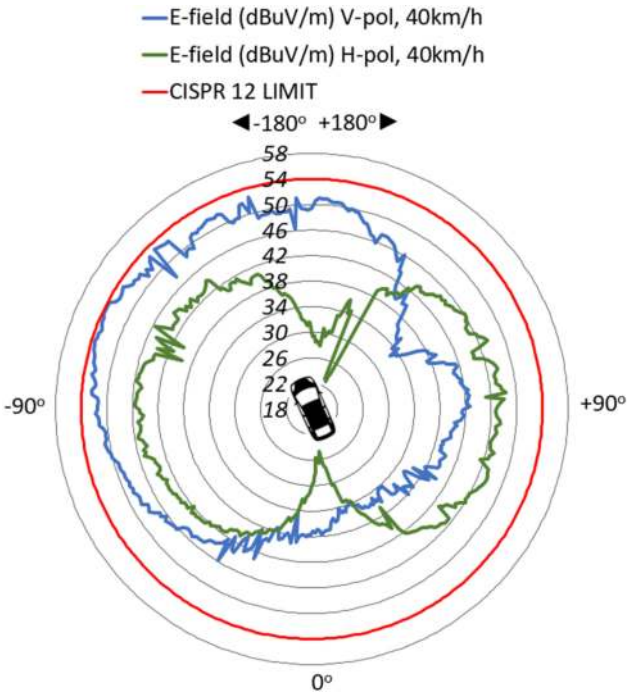

Fig. 4. E-field radiation pattern around the vehicle at 40 km/h on the vertical (blue trace) and horizontal (green trace) polarization.

the vehicle at a fixed frequency to identify the angle of the highest emission. For this purpose, the EMI receiver was configured to carry out an analysis at 33.5 MHz (fixed frequency), in order to extract the E-field radiation pattern around the vehicle. During this setup the vehicle was driven at a constant speed of 40 km/h with the antenna placed 3 m above the ground. The results of this measurement, for vertical and horizontal polarizations, are shown in Fig. 4, with the front side of the vehicle pointing at $-155°$.

From Fig. 4 it is evident that the level of the vertically polarized E-field around the vehicle at constant speed deviated almost by 21 dB, between the maximum ($\approx$54 dBμV/m) and the minimum value ($\approx$33 dBμV/m). The worst-case emissions for this setup, were captured toward the front-left area of the vehicle, at around $-120°$, from now on called as the "critical" angle, while the lowest emissions were noted on the rear and the right side of the vehicle. Upon further visual inspection inside the chassis of the vehicle, we noticed that the electric traction motor of the powertrain and the Hybrid Control Unit (HCU) were located on front-left of the engine compartment and as such this arrangement might have a relevance with the higher level emissions from this area. The values of the E-field, on the left ($-65°$) and right ($+115°$) side of the vehicle as considered by the test method under CISPR 12, were 50 and 38 dBμV/m, respectively, which were lower than the worst-case emission identified by the full 360° rotation for the vertical polarization.

Fig. 4 depicts the radiation pattern results when the antenna also was placed in horizontal polarization. The worst case emissions in this case was not more than 48 dBμV/m emitted on the front-left, same as in the vertical polarization, and right-rear area on the vehicle. The overall deviation level of the E-field

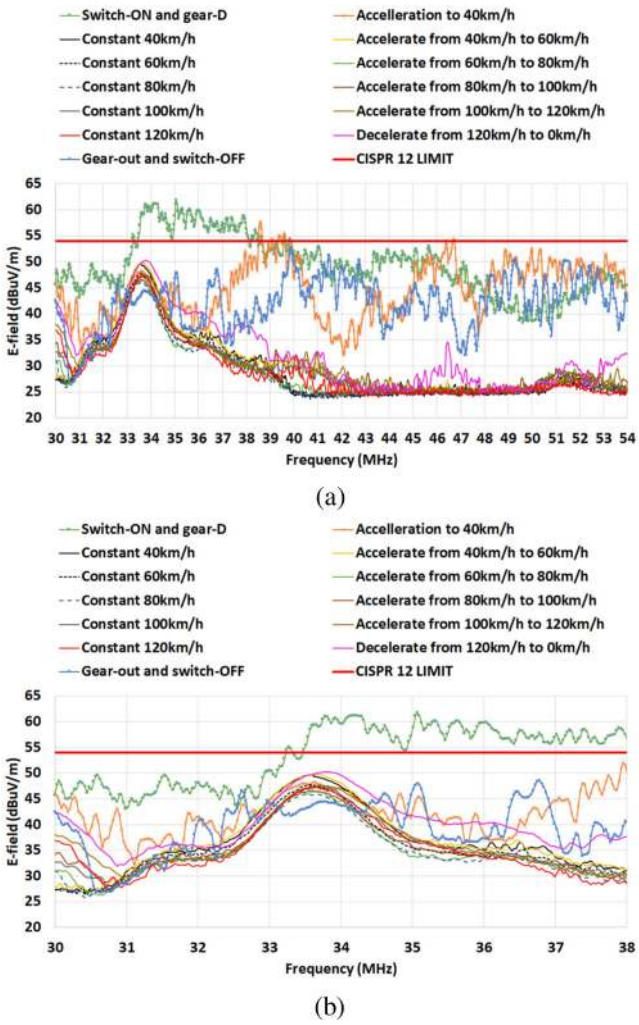

Fig. 5. Radiated emissions (vertical polarization and left side of the vehicle) during a complete drive cycle with stepped velocity (as per test method 3, Table VI) up to 120 km/h. (a) 30–54 MHz. (b) Close-in look 30–38 MHz.

was again significant, around 20 dB or so, justifying further the importance of a full 360° azimuth scan.

C. Impact of Intermediate Speeds on the Radiated Emissions

The next test block, based on test method 3 (Table II) constituted of several intermediate captures in the FD. For the purpose of identifying the worst-case emissions and apply the fastest frequency scan method around 33.48 MHz, the EMI receiver was set at 24 MHz frequency span between 30 and 54 MHz that was the maximum band utilized by the FFT calculation of the instrument.

Fig. 5(a) shows the measured E-field generated by the vehicle on the left side during each instance of test method 3 throughout the drive cycle, with the antenna placed in the vertical polarization and 3 m above the ground. From this figure, the level of radiated emissions were a function of vehicle's different constant speeds and deviated within 5 dB or so at around 33.48 MHz and by about 10 dB close to 30 MHz. Fig. 5(a), also showed that the frequency of the maximum emissions during the initial

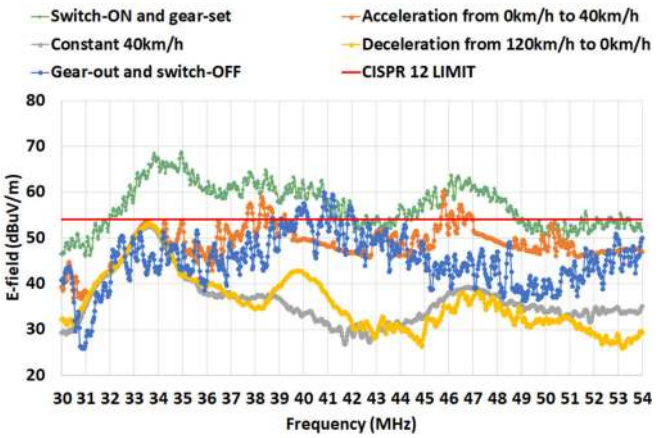

Fig. 6. Dominant radiated emissions with the turntable at the critical angle (vertical polarization and front-left side of the vehicle) during a complete stepped-speed drive cycle up to 120 km/h.

acceleration, from 0 to 40 km/h was at 38.6 MHz, which was different from the critical frequency identified during constant speed drive i.e., ≈33.5 MHz. Additionally, the switch-ON of the engine, the setting of the gear into D-position, i.e., drive contributed as well significantly to the overall emissions which exceeded the limit. At the end of the drive cycle, the emissions close to 33.5 MHz during the deceleration from 120 to 0 km/h (pink trace in Fig. 5(a)) exceeded those of all other driving instances and were even more pronounced during the "gear-out and switch-OFF" action.

Fig. 5(b) shows a close-up look (30–38 MHz) of the emissions centered around the critical frequency to visualize in more detail the critical emissions. In this figure, the level of the radiated emissions started from as low as 30 MHz indicating that the emissions could extend even lower than this band limit and also it was indicated that such emissions were predominately dominated by the dynamic (acc/tion, dec/tion, switch-ON, set gears) events of the vehicle. Specifically, the majority of these traces near the 30 MHz were related to the vehicles dynamic processes, e.g., driving the vehicle from 0 to 40 km/h, or from 80 to 100 km/h, or from 100 to 120 km/h, as well as switching ON and OFF the vehicle's engine. On the other hand, the levels of the emissions under constant speed driving close to 30 MHz were lower and in most cases were peaking around the 33.48 MHz.

The most critical events from the emissions point of view in Fig. 5 (switching-ON, acceleration and deceleration), were compared with these when the vehicle was tested again with the turntable angle set at the critical angle which was identified in Fig. 4 in the vertical polarization, i.e., the front-left area of the vehicle chassis. The measured results at this critical angle with the antenna in the vertical polarization and 3 m above the ground are shown in Fig. 6.

In Fig. 6, showing the driving events of the most critical emissions close or above the limit, the levels of the measured E-field were generally higher in this case, compared to the left side of the vehicle, Fig. 5(a). During "switch-ON and gear-out" the generated emissions at the front-left area of the vehicle were almost 9 dB higher than these at the left side (Fig. 5). In addition,

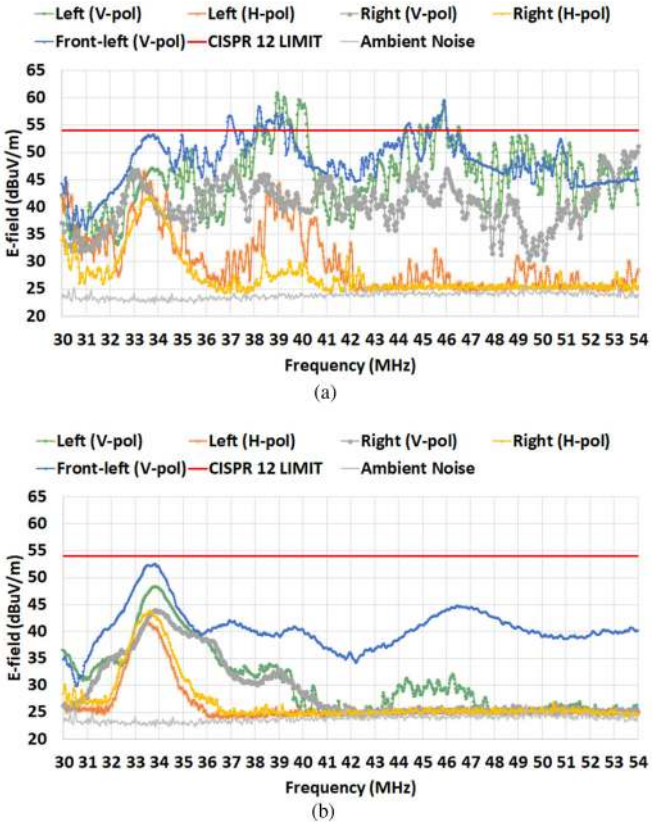

Fig. 7. Emission levels during aggressive (a) acceleration from 0 to 80 km/h and (b) deceleration from 80 to 0 km/h, for both polarizations on the left, right side, and vertical polarization on front-left of the vehicle.

"gear-out and switch-OFF" action exceeded as well the allowed limit in this case compared to the left side of the vehicle. At 40 km/h constant speed the emissions were marginally close to the limit, something which was not evident on the left side of the vehicle, as they were about 5 dB below this limit. It was also observed that the deceleration (120 to 0 km/h) process generated EM emissions which were higher by almost 5 dB than these during constant speed drive.

D. Impact of Aggressive Acceleration and Deceleration on the Radiated Emissions

In order to examine in more detail the association between that of the sudden acceleration, deceleration, and the radiated emissions, additional tests were carried out inside the SAC. In this set of experiments, the vehicle was driven up to 80 km/h according to the test method 4 (Table II). The results of the emissions on the left, right and front-left of the vehicle during the acceleration and deceleration instances are shown in Fig. 7(a) and (b), respectively.

In Fig. 7, the emissions in the vertical polarization were particularly high at the front-left and left side of the vehicle and less on the right side. The results are also well correlated with the radiation pattern plot in Fig. 4 which identified that the front-left area of the vehicle in the vertical polarization was the most critical for the emissions near 33.5 MHz. We also observed that during the acceleration and deceleration phases

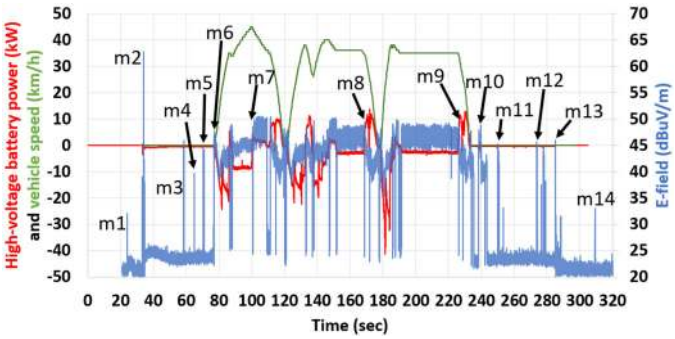

Fig. 8. Radiated emissions (vertical polarization and left-side of the vehicle), vehicle velocity and high-voltage traction-battery power during a drive cycle up to 45 km/h.

the EMI showed a broadband behavior covering the majority of the measured band. The emissions on the horizontal polarization were generally lower than those in the vertical polarization. From these traces it was seen that dynamic velocity variations had a strong impact on the interference levels generated by the vehicle.

E. Radiated Emissions Time Dependence During a Typical Drive Cycle

As a means to explore in more detail the time dependence of the EM emissions during a complete drive cycle, several laboratory tests were also carried out with the receiver locked into a fixed frequency, while the emissions were plotted as a function of time while the vehicle was at a fixed angle on the SAC turntable. For this purpose, the frequency at 33.48 MHz, which was identified as the most critical during the constant speed, was selected. Alternatively, if someone wanted to examine further the effect mainly of the acceleration, the frequency would need to be selected at 41, 39, or 46 MHz based on the peak emissions of the corresponding traces in Figs. 6 and 7.

Fig. 8 presents the results of this measurement in the time domain. In this case, the receive antenna was placed on the left side of the vehicle, 3 m above the ground and the vehicle speed was kept up to 45 km/h. A drive cycle within a 5 min measurement interval was considered to reflect typical driving events as in real life. During the measurement, additional parameters of the vehicle: 1) speed and 2) power consumption of the electric-traction vehicle battery, were also recorded. The test was also video-recorded to provide an additional tool for post-processing our findings and verify the sequence of the various events (switch-ON, gear change, braking, acc/tion, dec/tion, switch-OFF, etc.) in more detail.

Table V provides the timing information of the relevant markers indicated in Fig. 8. On Fig. 8, the negative (−) sign of the power values of the high-voltage traction battery vehicle referred to battery discharging, while a positive (+) sign identified a regenerative process during deceleration, which charged the high-voltage traction battery.

From Fig. 8, we can extract a number of important observations relating the radiated emissions of the vehicle with its operation during this drive cycle. It was seen that switching-ON

TABLE V
MAJOR INSTANCES OF THE VEHICLE OPERATION DURING A FIXED FREQUENCY TIME-SWEEP RADIATED EMISSIONS TEST FOR THE DRIVE CYCLE SHOWN ON FIG. 8 (GEARS: P = PARKING, R = REVERSE, N = NEUTRAL, D = DRIVE)

Marker (Fig. 8)	Event
m1	Brake pressed and remained pressed with engine-OFF
m2	Engine switch-ON
m3	Set gear-P to gear-R
m4	Set gear-R to gear-N
m5	Set gear-N to gear D
m6	Brake released and accelerator pressed
m7	Accelerator released, vehicle slowed down by free-wheeling
m8	Accelerator released and brake pressed
m9	Accelerator released and brake pressed
m10	Brake released (while on gear-D) and pressed 7 secs later
m11	Gear-D to N to R to P
m12	Driver's window up/down/up
m13	Engine switch-OFF
m14	Brake released

(market "m2") the electric engine and setting the gears (markers "m3," "m4," and "m5") in preparation for driving, generated significant EM disturbances, although these were short in duration. The release of the brake and the press of the accelerator (marker "m6"), after the vehicle was set on gear-D for driving generated sharp emissions, which decayed slowly but then these increased again in proportion to the vehicle speed during acceleration. Constant speed driving contributed too to the EM emissions and as long as the speed was kept constant the emissions had a relatively constant peak envelope response, as shown, e.g., between 200 and 220 s at around 35 km/h.

However, we have noticed that slowing down by breaking and slowing down by releasing the pressure from the accelerator, resulted in different levels of emissions. At the 100 s (m7) in Fig. 8 and up to around 110 s, the accelerator was released and the vehicle slowed down by free-wheeling due to the chassis dynamometer road load resistance effect and air-drag, without pressing the brake. In this situation, the maximum EM emissions increased and they actually exceeded those during a constant speed drive mode (200–220 s). This elevated level of emissions could be due to the internal regeneration process of the vehicle, which charged the battery trough the power management system. The press of the brake (m8) during driving in order to slow down the vehicle, e.g., between 170 and 180 s, did generate EM emissions, but to a lesser extent than in free-wheeling slowing down mode, although regeneration took place in both instances. This difference might be explained by the particularity of the vehicle's internal powertrain electric operations of the electric traction system during driving.

Another interesting observation concerned the action around marker "m10." After the final stop of the vehicle at around 232 s, while on gear-D and with the brake pressed (vehicle idle), the EM emissions were low. However, when the brake was released at "m10" these rise, while the gear is still on "D." This could be attributed to the activation of the electric traction system which was engaged in preparation for driving after the release of the brake. The effect of the operation of the driver's window is shown on marker "m12," which produced emissions that could

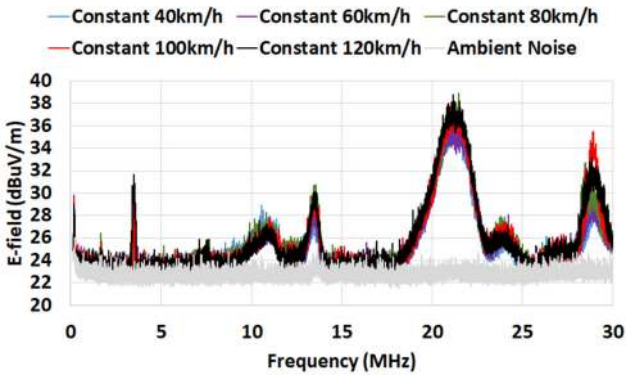

Fig. 9. 150 kHz to 30 MHz radiated emissions around the vehicle measured with an active monopole antenna at different constant speeds after a complete 360° azimuth scan.

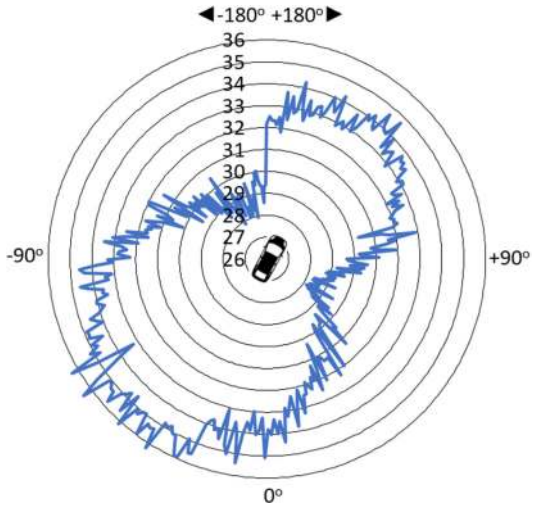

Fig. 10. E-field radiation pattern (21.08 MHz) around the vehicle at a constant speed (80 km/h).

be attributed to the electromechanical motor operation for the movement of the window glass.

F. Considerations for Other Frequency Bands

The PHEV was also tested for an exploratory point of view for its radiated emissions on frequency bands outside the standard 30–1000 MHz spectrum, focusing at: 1) 150–30 MHz and 2) 1–6 GHz, although no current European regulation obliges the automotive manufacturers to test the whole vehicle on these bands.

The definition of the various parameters configured into the scanning receiver instrument, were acquired from the experience with other automotive EMC standards related to the electric vehicles' charging infrastructure, such as IEC 61851-21-2 [28]. Within the latter standard the RBW for the frequency band at 150 kHz–30 MHz and 1–6 GHz was set at 9 kHz and 1 MHz, respectively, while the peak detector was employed in both frequency bands.

1) Radiated Emissions 150 kHz–30 MHz: The results of the peak radiated emissions for a full 360° scan while the vehicle was driven at different constant speeds (40, 60, 80, 100, 120 km/h) are presented in Fig. 9. For this set of measurements, an active monopole antenna was used, located 10 m away from the vehicle's side and distanced 1.40 m above the SAC floor.

From Fig. 9, it is seen that the spectrum below 30 MHz exhibited noticeable EM emissions with peaks at 184 kHz, 3.50 MHz, 10.55 MHz, 13.59 MHz, 21.08 MHz, and 28.83 MHz. The maximum peak emission exceeded 38 dBμV/m at 21.08 MHz, while the next peak was 35 dBμV/m at 28.83 MHz. As also shown in Fig. 9, the level of the emissions across the entire band was influenced by the vehicle speed, with the dominant peak observed at 21.08 MHz. At this frequency the measurement indicated that vehicle's emissions were influenced by the velocity, almost proportionally.

On the critical frequency 21.08 MHz, we carried out another test to plot the E-field radiation pattern of the vehicle during a constant speed of 80 km/h, with the results shown in Fig. 10.

In this setup the low frequency active monopole antenna inside the SAC was facing the front of the vehicle when the turntable was at +155°. From this plot, it was observed that the emissions were mainly dominant at the front (+155°) and the rear (−25°) side of the vehicle, with values reaching 34.5 and 36.5 dBμV/m, respectively. On the other hand, the emissions on the left and right side of the vehicle were lower, about 31 and 30 dBμV/m, respectively.

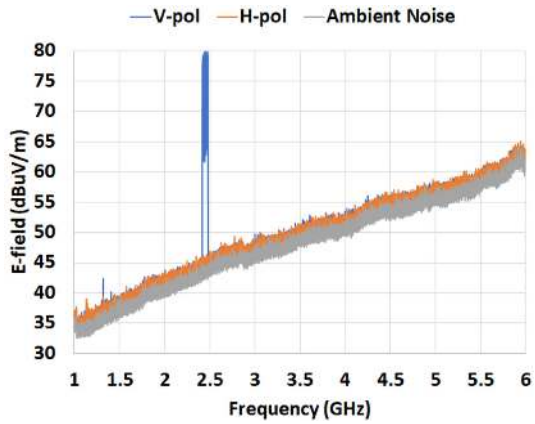

Fig. 11. 1–6 GHz radiated emissions around the vehicle at 80 km/h after a complete 360° azimuth scan.

2) Radiated Emissions 1–6 GHz: Unlike the radiated emissions from electric-vehicle charging systems as prescribed within, e.g., IEC 61851-21-2 standard [28], which includes compliance up to 6 GHz, CISPR 12 does not consider this higher frequency band. Fig. 11, shows the peak measured emissions of the vehicle with the antenna placed 3 m above the ground in both polarizations when it was driven at constant speed (80 km/h) during a full 360° rotation. Except at the frequency band from 2.41 to 2.48 GHz in the vertical polarization, the remainder of the spectrum remains unchanged with respect to the noise floor. It was noticed that the onboard Bluetooth feature of the vehicle was generating intermittent emissions on the 2.4 GHz band, during spectrum search on the ISM band for active devices (e.g.,

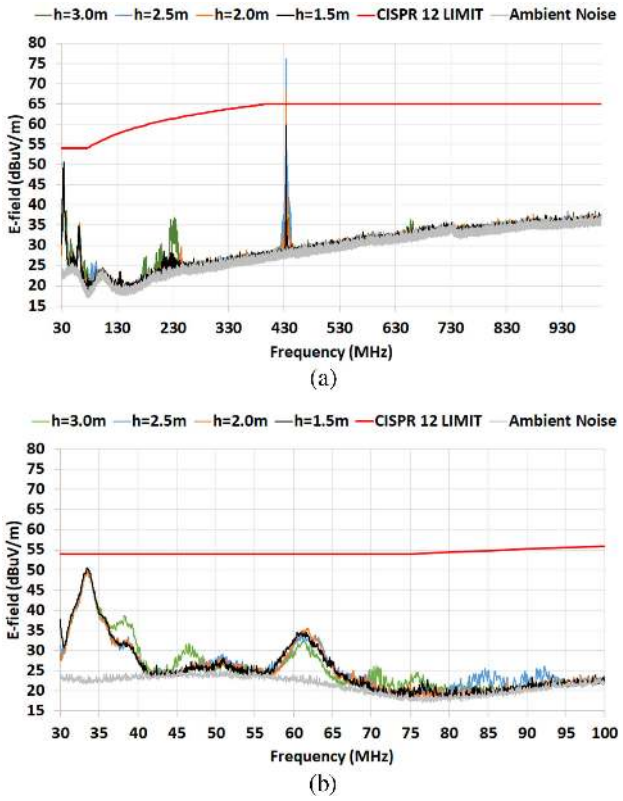

Fig. 12. Radiated emissions (vertical polarization) during a 360° scan at constant speed (80 km/h) with different receive antenna heights above the ground with frequency span. (a) 30–1000 MHz. (b) 30–100 MHz.

handsets, etc.). The source of this emission was verified by deactivating the Bluetooth feature, through the driver's touch panel. From Fig. 11, it is seen that the levels of the radiated emissions due to the Bluetooth module were exceptionally strong when this was activated.

G. Effect of Antenna Height Scan

Height scanning of the antenna was carried out between 1.5 to 3.0 m (limited by the height adjustment range of the antenna mast) in steps of 0.5 m in order to examine the maximum emissions during constant speed drive. Due to the limited time availability of the vehicle in our laboratory, this test was conducted (using the peak detector) when the vehicle was driven at one fixed speed (80 km/h) with the antenna vertically oriented, while the frequency between 30 MHz and 1 GHz was monitored during a full 360° scan around the vehicle. The results of the peak emissions around the vehicle during a 360° scan in the FD are shown in Fig. 12(a).

Fig. 12(b) displays a close-in look of the emissions around the critical frequency (33.50 MHz), which was captured during constant speed. From this plot, it is illustrated that the radiated emissions at different antenna heights reached similar levels to the case when the antenna is at 3.0 m above the ground. Actually, the peak level of the E-field at 33.5 MHz (critical frequency) is marginally higher at 1.5 and 2.0 m, respectively, than at 3.0 m as shown in Fig. 12(b). As pointed out previously, the interference

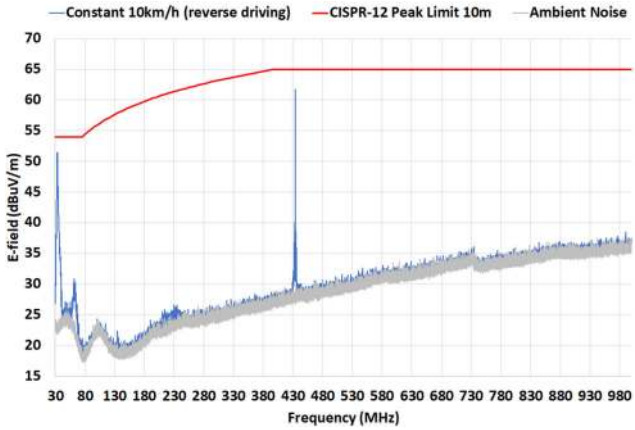

Fig. 13. Radiated emissions (vertical polarization) during a full 360° rotation at 10 km/h reverse speed.

at 433 MHz was due to a vehicle's onboard module system, which was active during driving.

H. Investigation of Reverse Driving on the Radiated Emissions

The impact of the reverse driving to the radiated emission was also briefly investigated. As the same electric motor was engaged during the reverse driving, it was expected to observe a similar interference profile across the 30–1000 MHz with that in the previous test configurations. The peak level of the emissions in the FD when the vehicle was driven at constant reverse speed of 10 km/h during a full 360° turntable rotation is depicted in Fig. 13. In this setup the antenna was vertically polarized and fixed at 3 m above the ground. The major interference was observed at 33.5 MHz and about 2.5 dB below the limit and its frequency value was correlated to the peak of Fig. 2(b) during forward driving.

I. Challenges and Constrains During the Measurements

As explained at the beginning, the scope of these experimental investigations was not to provide an exhaustive test matrix or check vehicle compliance, but rather to present practical EMC test methods on a vehicle based on real drive situations more closely. Additional measurements under different setups could have been conducted in this work. For example, various vehicle speeds, antenna polarization and heights could have been carried out on the 1–6 GHz and 150 kHz–30 MHz (only vertical polarization) bands. Furthermore, retaining an absolute constant speed during the tests for a prolonged time was also challenging for the driver, so minor speed deviations, i.e., ±3 km/h around the reference speed were inevitable.

IV. Conclusion and Suggestions for Future Work

The laboratory results presented in this article, based on nonlegislative measurement procedures, identified weaknesses in the existing automotive EMC emissions test methods. EMI generated by vehicles can be higher when real (dynamic) drive conditions and laboratory setups beyond the fixed setups prescribed on the current standards are considered. Observations

and conclusions described in this study are valid for the specific vehicle and testing conditions, while all measurements considered actual road-load resistance to resemble realistic situations.

Testing a vehicle under realistic scenarios, that is at different constant speeds, accelerations and decelerations, can result in the generation of radiated emissions, which are not revealed during one constant speed. The application of a full 360° (azimuth) scan around the vehicle showed that the worst-case emissions could be generated from any angle. Novel results also were presented that identified the association of vehicle speed and power consumption of the electric traction battery with the electromagnetic emissions in time and we demonstrated that real drive situations can have a significant impact on the actual level of radiated emissions. This brings up the need to consider the time-dependence of the E-field emissions by applying a dynamic drive-cycle during a vehicle's EMC testing as it is utilized, e.g., in the fuel emissions testing type-approval of vehicles. Moreover, it was shown that the frequencies of the EM disturbances generated by a vehicle can also extend above and below the conventional 30–1000 MHz frequency range. The test methods presented in this article can become a valuable evaluation tool during the EMC debugging and pre-compliance test phases of a vehicle.

APPENDIX

TABLE VI
VEHICLE TECHNICAL SPECIFICATIONS

Year of Production	2017
Powertrain type	Plug-in hybrid (PHEV)
Battery capacity of electric powertrain	9kWh (360V nominal voltage)
Battery composition	Li-Po
Power rating of the electric speed motor	45kW
Size of fuel engine	1600 cc

TABLE VII
EMC TEST EQUIPMENT

Antennas	
Schwarzbeck	VULB 9162 Broadband (30 - 8000 MHz)
ETS Lindgren	3301C Active Monopole (30 Hz - 50 MHz)
Cables	
SSB-Electronic	ECOFLEX-10
EMI Receiver	
Rohde and Schwarz	ESR7 (9 kHz – 7 GHz) with FFT option

TABLE VIII
SAC CHASSIS DYNAMOMETER SETTINGS

Parameter	**Chassis dynamometer road load factor**
Inertia (kg)	1807.5
F0 (N)	1.933
F1 (N/km/h)	0.08309
F2 (N/(km/h)^2)	0.050773

ACKNOWLEDGMENT

The authors would like to express their appreciation to G. Martini (Joint Research Centre, European Commission), A. Tansini (Joint Research Centre, European Commission), and A. Bonamin (AVL, Italy) for their valuable support and constructive discussions on this research campaign.

REFERENCES

[1] *UNECE Regulation 10*, Revision 6, Nov. 20, 2019. Accessed: Mar. 11, 2020. [Online]. Available: https://www.unece.org/fileadmin/DAM/trans/main/wp29/wp29regs/2019/E-ECE-324-Add.9-Rev.6.pdf

[2] *Vehicles, Boats and Internal Combustion Engines – Radio Disturbance Characteristics – Limits and Methods of Measurement for the Protection of Off-Board Receivers*, CISPR 12:2007+AMD1:2009 CSV, CISPR, Geneva, Switzerland.

[3] C. Christopoulos, *Principles and Techniques of Electromagnetic Compatibility*. 2nd ed. Boca Raton, FL, USA: CRC Press, 2007.

[4] M. I. Montorose and E. M. Nakauchi, *Testing for EMC Compliance: Approaches and Techniques*. Hoboken, NJ, USA: Wiley-IEEE Press, 2004.

[5] K. Armstrong, "Including EMC in risk assessments," in *Proc. IEEE Int. Symp. Electromagn. Compat.*, 2010, pp. 796–801.

[6] J. C. Lin, "Human exposure to RF, microwave, and millimeter-wave electromagnetic radiation," *IEEE Microw. Mag. Health Effects*, vol. 17, no. 6, pp. 32–36, Jun. 2016.

[7] *Directive 2004/104/EC of 14 October 2004 Adapting to Technical Progress Council Directive 72/245/EEC Relating to the Radio Interference (Electromagnetic Compatibility) of Vehicles and Amending Directive 70/156/EEC on the Approximation of the Laws of the Member States Relating to the Type-Approval of Motor Vehicles and Their Trailers*, Official Journal of the European Union, no. L 337, pp. 13–58, Nov. 13, 2004.

[8] *Vehicles', Motorboats' and Spark-Ignited Engine-Driven Devices' Radio Disturbance Characteristics – Limits and Methods of Measurement*, 5th ed. (2001) and Amd1 (2005), CISPR 12:2001+AMD1:2005, CISPR, Geneva, Switzerland.

[9] A. R. Ruddle, D. A. Topham, and D. D. Ward, "Investigation of electromagnetic emissions measurements practices for alternative powertrain road vehicles," in *Proc. IEEE Symp. Electromagn. Compat. Symp. Record (Cat. No.03CH37446)*, vol. 2, 2003, pp. 543–547.

[10] A. R. Ruddle, "Investigation of automotive emissions measurement frequencies, test methods and operating modes," in *Proc. 16th Zurich Int. EMC Symp.*, Zurich, Switzerland, Feb. 2005, pp. 115–120.

[11] M. Paterson and J. F Dawson, "An investigation into the errors in the CISPR 12 full vehicle radiated emissions measurements due to vehicle directivity," in *Proc. Int. Symp. Electromagn. Compat.*, 2013, pp. 310–315.

[12] C. Visvikis *et al.*, "Electric vehicles: review of type approval legislation and potential risks," TRL, Crowthorne, U.K., Report no. CPR 810, Jun. 2, 2010.

[13] R. Armstrong, L. Dawson, A. J. Rowell, C. A. Marshman, and A. R. Ruddle, "The effect of fully electric vehicles on the low frequency electromagnetic environment," in *Proc. IEEE Int. Symp. Electromagn. Compat. (EMC)*, 2015, pp. 662–667.

[14] A. R. Ruddle and R. Armstrong, "Review of current EMC standards in relation to vehicles with electric powertrains," in *Proc. Int. Symp. Electromagn. Compat.*, 2013, pp. 298–303.

[15] C. Chen, "Characterizing the generation & coupling mechanisms of electromagnetic interference noise from an electric vehicle traction drive up to microwave frequencies," in *Proc. APEC, 15th Annu. IEEE Appl. Power Electron. Conf. Expo. (Cat. No.00CH37058)*, vol. 2, 2000, pp. 1170–1176.

[16] M. Dong, L. Zhai, R. Gao, and X. Zhang, "Research on radiated electromagnetic interference (EMI) from power cables of a three-phase inverter for electric vehicles," in *Proc. IEEE Conf. Expo. Transp. Electrific. Asia-Pacific*, 2014, pp. 1–5.

[17] F. Silva and M. Aragón, "Electromagnetic interferences from electric/hybrid vehicles," in *Proc. Gen. Assem. Int. Union Radio Sci. Gen. Assem. Sci. Symp.*, 2011, pp. 1–4.

[18] *Electromagnetic Compatibility of Multimedia Equipment – Emission Requirements*, CISPR 32:2015, Mar. 2015.

[19] *Information Technology Equipment – Radio Disturbance Characteristics – Limits and Methods of Measurement*, CISPR 22:2008, Sep. 2008.

[20] T. Williams, *EMC for Product Designers*. 4th ed. New York, NY, USA: Elsevier Science, 2007.

[21] *Specifications for Radio Disturbance and Immunity Measuring Apparatus and Methods – Part 1–4: Radio Disturbance and Immunity Measuring Apparatus – Antennas and Test Sites for Radiated Disturbances mMasurements*, CISPR 16-1-4, 3rd ed., 2019.

[22] European Commission – Fact Sheet, "*Testing of emissions from cars*." Brussels, Belgium, May 4, 2018. Accessed: May 01, 2019. [Online]. Available: http://europa.eu/rapid/press-release_MEMO-18-3646_en.htm.
[23] B. Wangard, "How to significantly reduce EMI test time," in *Proc. IEEE Int. Symp. Electromagn. Compat., Signal Power Integrity, EMC+SIPI*, Washington, DC, USA, Aug. 2017.
[24] *Rohde and Schwarz ESR EMI Test Receiver Specifications (Version 06.00)*, 2017. Accessed: Feb. 02, 2019. [Online]. Available: https://www.rohde-schwarz.com/nl/product/esr-productstartpage_63493-17877.html
[25] Rohde and Schwarz White Paper "Comparison of time domain scans and stepped frequency scans in EMI test receivers," Jan. 2014. Accessed: May 01, 2019. [Online]. Available: https://www.rohde-schwarz.com/us/applications/comparison-of-time-domain-scans-and-stepped-frequency-scans-in-emi-test-receivers-white-paper_230854-54019.html
[26] V. Janssen, "RFI emission measurements: Current status on CISPR standards," Feb. 14, 2011. Accessed: Jul. 01, 2018. [Online]. Available: https://www.schurter.com/en/Documents-References/Downloads-Document-Request?SearchText=RFI+emission+measurements+Current+status+on+CISPRstandards&ResultsPerPage= 10&LanguageID=0&RegionID=0&CategoryID=0&SubcategoryID=0
[27] European Table of Frequency Allocations. Accessed: Mar. 11, 2020. [Online]. Available at: https://www.efis.dk/reports/ReportDownloader?reportid=1.
[28] *Electric Vehicle Conductive Charging System – Part 21-2: Electric Vehicle Requirements for Conductive Connection to an AC/DC Supply – EMC Requirements for Off Board Electric Vehicle Charging Systems*, IEC 61851-21-2:2018.

Konstantinos Pliakostathis received M.Eng. degree (hons.) in electronic systems engineering, in 2000, and the Ph.D degree in microwave antennas, in 2004, both from the Department of Electronic Systems Engineering, University of Essex, Colchester, Essex, U.K.

Currently he is a Scientific Research Officer with the E-Mobility Electromagnetic Testing Facilities at the Joint Research Centre of the European Commission, Italy. His areas of development include antennas, automotive EMC, EM scattering and propagation, and EMI troubleshooting test methodologies for electric/hybrid vehicles and their recharging infrastructure.

Marco Zanni received the degree in science of administration and organization of work from University of Turin, Campus L. Einaudi, Turin, Italy, in 2014.

From 1999 to 2017, he worked, in the private and public sector, in the field of electrical installation with particular focus in high and medium voltage distribution and grid interconnection/protection networks. Since the beginning of 2018, he has been working as Technical Responsible with the E-Mobility Electromagnetic Testing Facility at the Joint Research Centre, Ispra, Italy.

Germana Trentadue received her master's degree in telecommunications engineering from Politecnico of Bari, Italy in 2011. He studied telecommunications engineering at Politecnico of Bari, Bari, Italy.

Since 2014, she is a Laboratory Engineer with the European Commission's Joint Research Centre, Italy. She joined the JRC's Sustainable Transport Unit in 2016 and is part of the Unit's E-mobility Team and is involved in EVs and HEVs performance testing.

Harald Scholz studied mechanical engineering at Bochum (R.U.B.) and Karlsruhe, and received the Ph.D. degree from University of Karlsruhe, Germany, in 1997.

After working shortly for University of Karlsruhe, he joined ECâ's DG Research in late 1997 and ECâ's Joint Research Centre (JRC) in 2001. Since 2011, he has led the development of the electromobility laboratories, interoperability- and EMC- testing. He is currently coordinating the European Interoperability Centre for Electric Vehicles and Smart Grids as a Project Leader at the European Commissionâ's JRC in Ispra, Italy.